Matrix Infrared Spectroscopic and Theoretical Studies on the Reactions of Late Lanthanoid Atoms with Nitrous Oxide in Excess Argon

Ling Jiang and Qiang Xu*

National Institute of Advanced Industrial Science and Technology (AIST), Ikeda, Osaka 563-8577, Japan

Received: October 29, 2008; Revised Manuscript Received: January 29, 2009

Reactions of laser-ablated late lanthanoid atoms (Gd, Tb, Dy, Ho, Er, Tm, Yb, and Lu) with N_2O molecules in excess argon have been investigated using matrix-isolation infrared spectroscopy. Lanthanoid monoxide−dinitrogen complexes, $OLn(N_2)$ and OLnNN, are observed for Gd, Tb, Ho, and Er, and the $OLnNN^+$ cations are observed for Gd to Lu except for Yb. The new products are characterized on the basis of isotopic shifts, mixed isotopic splitting patterns, and CCl_4-doping experiments. Density functional theory calculations have been performed on the new species, which support identification of the $OLn(N_2)$, OLnNN, and $OLnNN^+$ complexes from the matrix infrared spectra. Together with our earlier work involving early lanthanoid atoms, several trends are identified for the reactions of lanthanoid atoms with N_2O molecules.

Introduction

The chemistry of lanthanoid (Ln) atoms with small molecules (i.e., N_2O, CO, N_2, O_2, NO, H_2, H_2O, CO_2, etc.) has been the subject of considerable studies both in gas-phase and rare-gas matrixes as pointed out previously.[1−9] Taking the CO ligand as an example, matrix investigations have characterized several binary lanthanide metal carbonyls, $Ln(CO)_x$ ($x = 1-6$).[3] In particular, the lanthanide dimers react with CO to form a new series of the $Ln_2[\eta^2(\mu_2\text{-C, O})]$ complexes with asymmetrically bridging and side-on-bonded CO ligands, which exhibit unusually low C−O stretching frequencies and offer a structural configuration of the precursor to CO dissociation.[3e−h] The reactions of lanthanoid atoms with isoelectronic N_2 molecule produced a series of nitride and dinitrogen complexes, LnN, $(LnN)_2$, $Ln(N_2)$, Ln(NN), and $Ln(NN)_2$.[4a] Interestingly, the Gd_2 dimer reacts with N_2 in solid argon to form a homoleptic dinuclear dinitrogen complex $[Gd_2(\mu\text{-}\eta^2\text{:}\eta^1\text{-}N_2)]$ containing a drastically activated side-on and end-on bonded N_2 ligand.[3] This complex rearranges to a planar cyclic $[Gd(\mu\text{-}N)_2Gd]$ isomer with a completely cleaved N−N bond and further dimerizes to form a unique cubic (Gd_4N_4) cluster.[4b]

Recent studies on the reactions of early lanthanoid atoms (La−Eu) with N_2O in excess argon have identified a series of the metal monoxide−dinitrogen ($OLn(N_2)$) and $OLnNN^+$ (Ln = La, Ce, Pr, Nd, and Sm) complexes.[2b,c] Here, we report a study of the reactions of late lanthanoid atoms (Gd−Lu) with N_2O in excess argon. Infrared spectroscopy coupled with quantum chemical calculation provides evidence for the formation of the metal monoxide−dinitrogen complexes, $OLn(N_2)$ and OLnNN (Ln = Gd, Tb, Ho, and Er), and the $OLnNN^+$ (Ln = Gd−Lu except for Yb) cation complexes. The present results are compared with our previous study on the reactions of N_2O with early lanthanoid atoms to explore the trends in the chemistry of lanthanoid atoms with N_2O.

Experimental and Theoretical Methods

Experiments for laser ablation and matrix-isolation infrared spectroscopy are similar to those previously reported.[10] In short, the Nd:YAG laser fundamental (1064 nm, 10 Hz repetition rate with 10 ns pulse width) was focused on the rotating late lanthanoid (Gd, Tb, Dy, Ho, Er, Tm, Yb, and Lu) (99.9%, Kojundo Chemical Laboratory Co.) targets. The laser-ablated lanthanoid atoms were codeposited with N_2O in excess argon onto a CsI window cooled normally to 4 K by means of a closed-cycle helium refrigerator. Typically, 1−20 mJ/pulse laser power was used. N_2O (99.5%, Taiyo Nippon Sanso Co.), $^{15}N_2O$ (98%, Cambridge Isotopic Laboratories), and $^{14}N_2O + {}^{15}N_2O$ mixtures were used in different experiments. In general, matrix samples were deposited for 30−60 min with a typical rate of 2−4 mmol per hour. After sample deposition, IR spectra were recorded on a BIO-RAD FTS-6000e spectrometer at 0.5 cm^{-1} resolution using a liquid nitrogen cooled HgCdTe (MCT) detector for the spectral range of 5000−400 cm^{-1}. Samples were annealed at different temperatures and subjected to broadband irradiation ($\lambda > 250$ nm) using a high-pressure mercury arc lamp (Ushio, 100 W).

Density functional theory (DFT) calculations were performed to predict the structures and vibrational frequencies of the observed reaction products using the Gaussian 03 program.[11] All the present computations employed the BP86 density functional method.[12] The 6-311+G(d) basis set was used for the N and O atoms,[13] and the scalar-relativistic SDD pseudopotential and basis set were used for the lanthanoid atoms.[14] Geometries were fully optimized and vibrational frequencies were calculated with analytical second derivatives. Earlier investigations have shown that such computational methods can provide reliable information for metal complexes, such as infrared frequencies, relative absorption intensities, and isotopic shifts.[2,8]

Results and Discussion

Experiments have been done with different concentrations of N_2O ranging from 0.02% to 2.0% in excess argon. Typical infrared spectra for the reactions of laser-ablated Gd atoms with N_2O molecules in excess argon in the selected regions are illustrated in Figures 1 and 2. The spectra of the other lanthanoid atoms are shown as Supporting Information. The absorption bands in different isotopic experiments are listed in Table 1.

* To whom correspondence should be addressed. E-mail: q.xu@aist.go.jp.

10.1021/jp809549u CCC: $40.75
Published on Web 03/09/2009

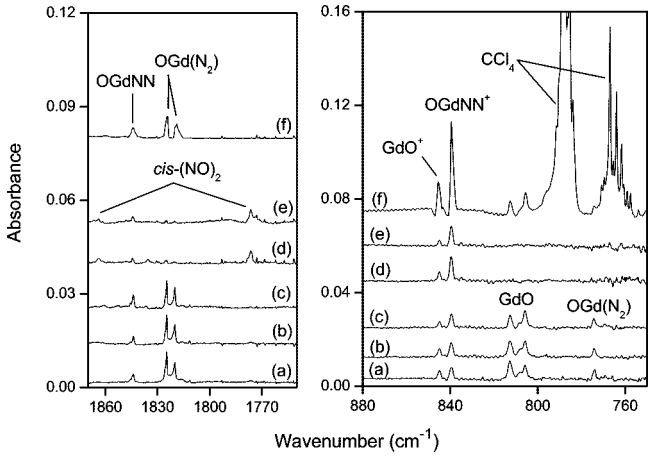

Figure 1. Infrared spectra in the 1860−1770 and 880−760 cm^{-1} regions from codeposition of laser-ablated Gd atoms with 0.4% N_2O in Ar at 4 K: (a) spectrum obtained from initial deposited sample for 1 h, (b) spectrum after annealing to 25 K, (c) spectrum after annealing to 30 K, (d) spectrum after 10 min of broadband irradiation, (e) spectrum after annealing to 35 K, and (f) spectrum obtained by depositing laser-ablated Gd atoms with 0.4% N_2O + 0.03% CCl_4 in Ar at 4 K for 1 h and annealing to 30 K.

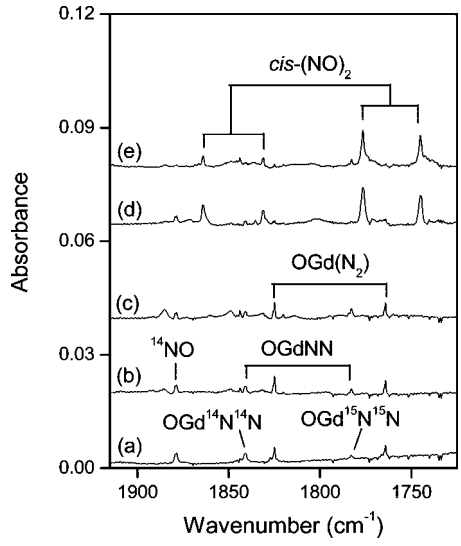

Figure 2. Infrared spectra in the 1900−1750 cm^{-1} region from codeposition of laser-ablated Gd atoms with 0.2% $^{14}N_2O$ + 0.2% $^{15}N_2O$ in Ar at 4 K. For the meaning of a−e, see Figure 1

The stepwise annealing and irradiation behavior of the product absorptions is also shown in the figures and will be discussed below. Experiments have also been done with different concentrations of CCl_4 serving as an electron scavenger.[15]

Quantum chemical calculations have been carried out for the possible isomers and electronic states of the species involved in the Ln + N_2O reactions. DFT calculations show that the optimized structures of the isomers for Gd to Lu are similar to those for Sc, Y, and La.[2] Herein, only the calculated results of the observed products are presented for discussion. Figure 3 shows the optimized structures of the products. The comparison of the observed and calculated IR frequencies and isotopic frequency ratios for the N−O and Ln−O stretching modes of the products are summarized in Table 2. The ground electronic states, point groups, vibrational frequencies, and intensities of the products are listed in Table 3. The comparison of the Ln−O stretching frequencies for the LnO, $OLn(N_2)$, LnO^+, and $OLnNN^+$ complexes is given in Table 4. Natural electron configurations of lanthanoid atoms in the $OLn(N_2)$ complexes are reported in Table 5.

TABLE 1: IR Absorptions (in cm^{-1}) Observed from Codeposition of Laser-Ablated Late Lanthanoid Atoms (Gd−Lu) with N_2O in Excess Argon at 4 K

$^{14}N_2O$	$^{15}N_2O$	$^{14}N_2O$ + $^{15}N_2O$	$^{14}N_2O/^{15}N_2O$	assignment
1843.9	1782.7	1843.9, 1782.7	1.0343	OGdNN
1824.8	1764.0	1824.8, 1764.0	1.0345	$OGd(N_2)$
839.5	839.5		1.0000	$OGdNN^+$
774.4	774.4		1.0000	$OGd(N_2)$
1838.8	1777.9	1838.8, 1777.9	1.0343	OTbNN
1818.7	1758.2	1818.7, 1758.2	1.0344	$OTb(N_2)$
851.2	851.2		1.0000	$OTbNN^+$
786.6	786.6		1.0000	$OTb(N_2)$
855.9	855.9		1.0000	$ODyNN^+$
1844.9	1783.5	1844.9, 1783.5	1.0344	OHoNN
1816.8	1756.3	1816.8, 1756.3	1.0344	$OHo(N_2)$
855.1	855.1		1.0000	$OHoNN^+$
790.6	790.6		1.0000	$OHo(N_2)$
1849.2	1787.7	1849.2, 1787.7	1.0344	OErNN
1810.9	1750.6	1810.9, 1750.6	1.0344	$OEr(N_2)$
855.8	855.8		1.0000	$OErNN^+$
800.2	800.2		1.0000	$OEr(N_2)$
859.0	859.0		1.0000	$OTmNN^+$
862.1	862.1		1.0000	$OLuNN^+$

A. $OLn(N_2)$ and OLnNN (Ln = Gd, Tb, Ho, Er). In the reaction of Gd atoms with N_2O in the argon matrix, two absorptions at 1824.8 and 774.4 cm^{-1} appear together during sample deposition, change little after sample annealing, but decrease visibly upon broadband irradiation, and do not recover after further annealing to 35 K (Table 1 and Figure 1). The upper band at 1824.8 cm^{-1} shifts to 1764.0 cm^{-1} with $^{15}N_2O$, exhibiting an isotopic frequency ratio ($^{14}N_2O/^{15}N_2O$, 1.0345) characteristic of a N−N stretching vibration. The mixed $^{14}N_2O$

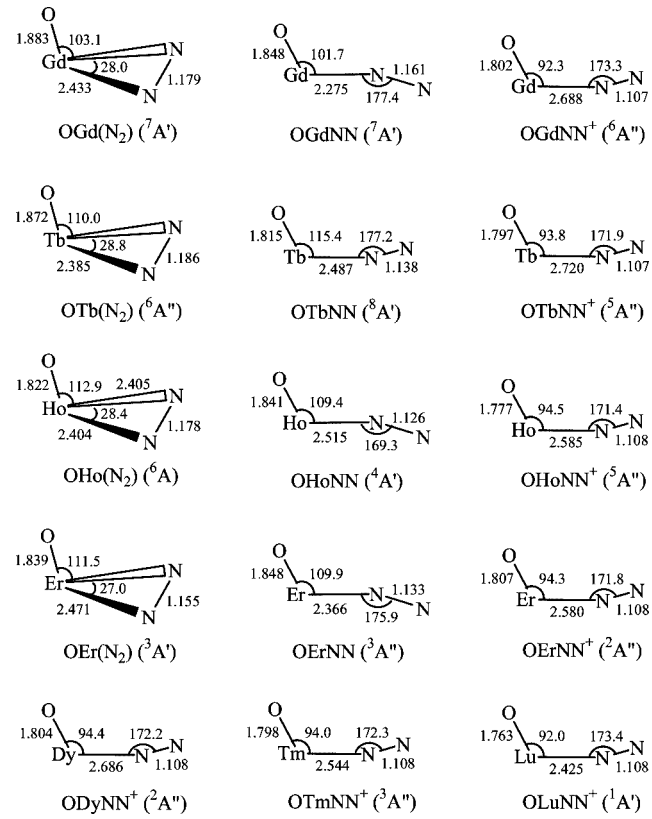

Figure 3. Optimized structures (bond lengths in angstroms, bond angles in degrees) of the products.

TABLE 2: Comparison of Observed and Calculated IR Frequencies (in cm^{-1}) and Isotopic Frequency Ratios for the Products

species	vibrational mode	observed		calculated	
		freq	$^{14}N_2O/^{15}N_2O$	freq	$^{14}N_2O/^{15}N_2O$
$OGd(N_2)$	ν_{N-N}	1824.8	1.0345	1837.5	1.0350
	ν_{Gd-O}	774.4	1.0000	700.9	1.0000
OGdNN	ν_{N-N}	1843.9	1.0343	1892.2	1.0350
$OTb(N_2)$	ν_{N-N}	1818.7	1.0344	1767.0	1.0350
	ν_{Tb-O}	786.6	1.0000	639.5	1.0000
OTbNN	ν_{N-N}	1838.8	1.0343	2051.2	1.0350
$OHo(N_2)$	ν_{N-N}	1816.8	1.0344	1841.5	1.0350
	ν_{Ho-O}	790.6	1.0000	752.5	1.0000
OHoNN	ν_{N-N}	1844.9	1.0344	2086.9	1.0350
$OEr(N_2)$	ν_{N-N}	1810.9	1.0344	1955.5	1.0350
	ν_{Er-O}	800.2	1.0000	764.1	1.0000
OErNN	ν_{N-N}	1849.2	1.0344	1908.0	1.0350
$OGdNN^+$	ν_{Gd-O}	839.5	1.0000	716.8	1.0000
$OTbNN^+$	ν_{Tb-O}	851.2	1.0000	728.7	1.0000
$ODyNN^+$	ν_{Dy-O}	855.9	1.0000	684.8	1.0000
$OHoNN^+$	ν_{Ho-O}	855.1	1.0000	818.2	1.0000
$OErNN^+$	ν_{Er-O}	855.8	1.0000	709.2	1.0000
$OTmNN^+$	ν_{Tm-O}	859.0	1.0000	730.1	1.0000
$OLuNN^+$	ν_{Lu-O}	862.1	1.0000	877.3	1.0000

+ $^{15}N_2O$ isotopic spectra (Figure 2) only provide the sum of pure isotopic bands, which indicates only one N_2 unit is involved in the complex.[16] The 774.4 cm^{-1} band, which is in the spectral range expected for the terminal Gd−O stretching mode,[5b] shows no nitrogen isotopic shift. The present spectra also show that the behavior with annealing and irradiation of another band at 1843.9 cm^{-1} is similar to that of the absorption at 1824.8 cm^{-1} (Figure 1). Furthermore, doping with CCl_4 has no effect on these bands (Figure 1, trace f), suggesting that these products are neutral.[15]

BP86 calculations indicate that the $OGd(N_2)$ complex is the most stable isomer, followed by the OGdNN complex, which lies only 1.66 kcal/mol above $OGd(N_2)$ (Figure 3). The N−N stretching vibrational frequencies in the $OGd(N_2)$ and OGdNN complexes are calculated to be 1837.5 and 1892.2 cm^{-1} (Table 3), respectively. The features of the IR spectra in the present matrix experiments are reminiscent of those of the side-bonded structure of $OSc(N_2)$ and end-on-bonded structure of OScNN, in which the corresponding N−N stretching vibrational frequencies appear at 1817.2 and 1849.2 cm^{-1} in excess argon,[2a] respectively. Accordingly, the 1824.8 and 774.4 cm^{-1} bands are assigned to the N−N and Gd−O stretching vibrations of the neutral $OGd(N_2)$ complex and the 1843.9 cm^{-1} band to the corresponding vibration of the neutral OGdNN complex on the basis of the results of the isotopic substitution, the N_2O concentration change, CCl_4-doping experiments, and the comparison with theoretical predictions. The Gd−O stretching vibration of the neutral OGdNN complex is absent from the present experiment.

The Gd−O stretching vibration in $OGd(N_2)$ is predicted to be 700.9 cm^{-1} (Table 3), which is 73.5 cm^{-1} below the experimental value of 774.4 cm^{-1}. Such large deviation for the Gd−O stretching vibrational frequency may be due to the inefficiency of the XC functional and/or the basis sets used here, posing a formidable theoretical challenge due to the large numbers of *f*-electrons and strong relativistic effects.[17−20] The intensity of the Gd−O stretching vibration in OGdNN is predicted to be about 1/3 that of the N−N stretching vibration, which is consistent with the absence of the Gd−O stretching vibration of the neutral OGdNN complex from the present experiment. As listed in Table 2, the calculated $^{14}N_2O/^{15}N_2O$ isotopic frequency ratios for the N−N and Gd−O stretching vibrations are also in accord with the experimental values. These agreements between the experimental and calculated vibrational frequencies, relative absorption intensities, and isotopic shifts confirm the identifications of the $OGd(N_2)$ and OGdNN complexes from the matrix IR spectra.

In the reactions of N_2O with the other late lanthanoid atoms, the absorptions of the analogous $OLn(N_2)$ and OLnNN complexes have been observed for Tb, Ho, and Er (Table 1 and Figures S1−S9 in the Supporting Information) but not for Dy, Tm, Yb, and Lu. The N−N and Ln−O stretching vibrations of $OLn(N_2)$ appear at 1818.7 and 786.6 cm^{-1} for Tb, 1816.8 and 790.6 cm^{-1} for Ho, and 1810.9 and 800.2 cm^{-1} for Er, respectively. The N−N stretching vibrations of OLnNN appear at 1838.8 cm^{-1} for Tb, 1844.9 cm^{-1} for Ho, and 1849.2 cm^{-1} for Er, respectively. DFT calculations predict that the $OLn(N_2)$ (Ln = Tb, Ho, and Er) complexes have $^6A''$, ^6A, and $^3A'$ ground states and the OLnNN (Ln = Tb, Ho, and Er) complexes have $^8A'$, $^4A'$, and $^3A''$ ground states (Figure 3), respectively. The calculated N−N and Ln−O stretching frequencies are consistent with the observed values (Tables 2 and 3). Furthermore, overall agreements between the experimental and calculated $^{14}N_2O/^{15}N_2O$ isotopic frequency ratios have also been obtained for the N−N and Ln−O stretching frequencies of the $OLn(N_2)$ and OLnNN complexes (Table 2).

B. $OLnNN^+$ (Ln = Gd, Tb, Dy, Ho, Er, Tm, Lu). Taking the Gd + N_2O reaction as an example, the absorption at 839.5 cm^{-1} appears during sample deposition, changes little after annealing, and increases markedly upon broadband irradiation at the expense of the neutral $OGd(N_2)$ and OGdNN complexes (Table 1 and Figure 1), indicating that this new species also has the GdN_2O stiochiometry. The band at 839.5 cm^{-1}, which is in the spectral range expected for the terminal Gd−O stretching mode,[5b] shows no nitrogen isotopic shift. Doping with CCl_4 sharply increases this band (Figure 1, trace f), suggesting that the product is cationic.[15] Although the 839.5 cm^{-1} band is only 5.3 cm^{-1} red-shifted from the Gd−O stretching vibration of the GdO^+ cation (844.8 cm^{-1}),[5b] the behavior of sample annealing and irradiation for the 839.5 cm^{-1} band is different from that for the 844.8 cm^{-1} band of the GdO^+ cation (Figure 1). By analogy with the $OMNN^+$ (M = Sc, Y, La, Ce, Pr, Nd, and Sm) spectra,[2] the 839.5 cm^{-1} band is assigned to the Gd−O stretching mode of the $OGdNN^+$ cation.

The $OGdNN^+$ complex is predicted to have a $^6A''$ ground-state with C_s symmetry (Table 3 and Figure 3). The calculated Gd−O stretching mode is 716.8 cm^{-1} (Table 2). The N−N stretching vibration is predicted to be 2344.7 cm^{-1} (Table 3). With its small intensity (19 km/mol), it is not likely to be observed, which is consistent with the absence from the present experiments.

In the reactions of N_2O with the other late lanthanoid atoms, the absorptions of the analogous $OLnNN^+$ (Ln = Tb, Dy, Ho, Er, Tm, and Lu) complexes have been observed in the region of 900−800 cm^{-1} (Tb, 851.2; Dy, 855.9; Ho, 855.1; Er, 855.8; Tm, 859.0; Yb, 840.1; Lu, 862.1 cm^{-1}) (Table 1 and Figures S1−S9 in the Supporting Information) but not for Yb.

BP86 calculations predict the $OLnNN^+$ (Ln = Tb, Dy, Ho, Er, Tm, and Lu) complexes to have $^5A''$, $^4A'$, $^5A''$, $^2A''$, $^3A''$, and $^1A'$ ground states with C_s symmetry (Figure 3), respectively. Overall agreements between the experimental and calculated vibrational frequencies, relative absorption intensities, and isotopic shifts have been obtained for the Ln−O stretching vibrations (Tables 2 and 3), respectively. It is noted that the Ln−O and N−N distances in the $OLnNN^+$ (Ln = Gd, Tb, Ho,

TABLE 3: Ground Electronic States, Point Groups, Vibrational Frequencies (in cm^{-1}) and Intensities (km/mol) of the Products

species	elec state	point group	frequency (intensity, mode)
$OGd(N_2)$	$^7A'$	C_s	1837.5 (143, A′), 700.9 (125, A′), 305.4 (26, A′), 295.4 (12, A″), 158.4 (1, A″), 116.3 (10, A′)
OGdNN	$^7A'$	C_s	1892.2 (378, A′), 677.2 (108, A′), 316.0 (14, A′), 229.2 (1, A′), 221.4 (27, A"), 94.2 (12, A′)
$OTb(N_2)$	$^6A''$	C_1	1767.0 (307, A′), 639.5 (71, A′), 294.5 (15, A″), 280.4 (4, A′), 161.4 (2, A″), 130.9 (16, A′)
OTbNN	$^8A'$	C_s	2051.2 (672, A'), 784.3 (306, A′), 188.7 (1, A′), 156.2 (1, A′), 91.1 (3, A″), 68.1 (22, A′)
$OHo(N_2)$	^6A	C_1	1841.5 (205, A), 752.5 (153, A), 317.4 (22, A), 313.2 (20, A), 149.0 (16, A), 140.5 (7, A)
OHoNN	$^4A'$	C_s	2086.9 (2173, A′), 736.8 (247, A′), 198.7 (10, A′), 156.0 (6, A′), 110.8 (3, A″), 99.8 (45, A′)
$OEr(N_2)$	$^3A'$	C_s	1955.5 (416, A′), 764.1 (281, A′), 281.8 (3, A″), 248.9 (2, A′), 175.2 (0.3, A″), 133.6 (23, A′)
OErNN	$^3A''$	C_s	1908.3 (7186, A′), 734.3 (197, A′), 222.8 (25, A′), 201.3 (78, A′), 139.5 (2, A″), 76.8 (7, A′)
$OGdNN^+$	$^6A''$	C_s	2344.7 (19, A′), 716.8 (64, A′), 189.2 (3, A′), 155.5 (1, A″), 151.8 (11, A′), 90.4 (12, A′)
$OTbNN^+$	$^5A''$	C_s	2345.8 (19, A′), 762.7 (65, A′), 181.6 (4, A′), 147.5 (16, A′), 139.4 (1, A″), 108.0 (8, A′)
$ODyNN^+$	$^4A'$	C_s	2342.6 (13, A′), 684.8 (46, A′), 193.1 (3, A′), 166.9 (1, A″), 151.3 (15, A′), 116.1 (6, A′)
$OHoNN^+$	$^5A''$	C_s	2341.2 (10, A′), 818.2 (100, A′), 211.0 (11, A′), 185.9 (12, A′), 171.9 (2, A″), 140.0 (7, A′)
$OErNN^+$	$^2A''$	C_s	2338.7 (7, A′), 709.2 (64, A′), 233.6 (11, A′), 190.4 (3, A′), 165.0 (2, A″), 160.0 (0.2, A′)
$OTmNN^+$	$^3A''$	C_s	2337.7 (7, A′), 730.1 (65, A′), 213.4 (3, A′), 176.5 (5, A′), 163.3 (2, A″), 79.4 (24, A′)
$OLuNN^+$	$^1A'$	C_s	2331.5 (5, A′), 877.3 (78, A′), 243.9 (7, A′), 206.7 (3, A′), 181.9 (1, A″), 91.6 (28, A′)

TABLE 4: Comparison of the Ln−O Stretching Frequencies (in cm^{-1}) for the LnO, $OLn(N_2)$, LnO^+, and $OLnNN^+$ Complexes

Ln	LnO	ref	$OLn(N_2)$	ref	LnO^+	ref	$OLnNN^+$	ref
La	796.7	5a	759.4	2b	838.2	5a	832.8	2b
Ce	808.3	5b	768.0	2c	849.4	5b	844.4	2c
Pr	816.9	5b	772.6	2c	857.4	5b	848.2	2c
Nd	825.1	5b	771.6	2c	878.4	5b	844.3	2c
Sm	807.4	5b	760.8	2c	840.0	5b	835.3	2c
Eu	667.8	5b			756.9	5b		
Gd	812.7	5b	774.4	this work	844.8	5b	839.5	this work
Tb	823.9	5c	786.6	this work	856.5	5c	851.2	this work
Dy	839.0	5c			888.6	5c	855.9	this work
Ho	838.1	5c	790.6	this work	887.9	5c	855.1	this work
Er	828.5	5c	800.2	this work	861.8	5c	855.8	this work
Tm	832.0	5c			864.2	5c	859.0	this work
Yb	660.0	5c			788.7	5c		
Lu	829.3	5c			864.9	5c	862.1	this work

TABLE 5: Natural Electron Configurations of Lanthanoid Atoms in the $OLn(N_2)$ Complexes

atom	natural electron configuration
La	[core] 6s(0.05) 4f(0.23) 5d(0.73) 6p(0.05) 5f(0.01) 6d(0.01)
Ce	[core] 6s(0.05) 4f(1.31) 5d(0.71) 6p(0.04) 5f(0.01) 6d(0.01)
Pr	[core] 6s(0.06) 4f(2.54) 5d(0.57) 6p(0.04) 5f(0.01)
Nd	[core] 6s(0.05) 4f(3.53) 5d(0.61) 6p(0.05)
Sm	[core] 6s(0.04) 4f(5.71) 5d(0.53) 6p(0.05)
Eu[a]	[core] 6s(0.05) 4f(6.79) 5d(0.48) 6p(0.06)
Gd	[core] 6s(0.47) 4f(7.07) 5d(0.54) 6p(0.03) 7s(0.03) 5f(0.01) 6d(0.01)
Tb	[core] 6s(0.70) 4f(7.91) 5d(0.48) 6p(0.02) 7s(0.02) 5f(0.01) 6d(0.01)
Dy[a]	[core] 6s(0.96) 4f(8.84) 5d(0.55) 6p(0.04) 7s(0.02) 5f(0.01)
Ho	[core] 6s(0.06) 4f(10.29) 5d(0.64) 6p(0.04) 5f(0.01)
Er	[core] 6s(0.06) 4f(11.51) 5d(0.52) 6p(0.05) 5f(0.01)
Tm[a]	[core] 6s(0.07) 4f(12.64) 5d(0.47) 6p(0.05)
Yb[a]	[core] 6s(0.07) 4f(13.51) 5d(0.40) 6p(0.03)
Lu[a]	[core] 6s(0.13) 5d(1.18) 6p(0.04) 5f(0.01) 6d(0.01)

[a] These $OLn(N_2)$ complexes are absent from the present matrix experiments.

and Er) complexes are slightly shorter than those in the $OLn(N_2)$ and OLnNN complexes, whereas the Ln−N distances in the $OLnNN^+$ complexes are longer than those in the $OLn(N_2)$ and OLnNN complexes (Figure 3).

C. Reaction Mechanism and Periodic Trend. On the basis of the behavior of sample annealing and irradiation, together with the observed species and calculated stable isomers, a plausible reaction mechanism can be proposed as follows. Under the present experimental conditions, the $OLn(N_2)$ and OLnNN (Ln = Gd, Tb, Ho, and Er) complexes are the primary products during sample deposition (Figure 1 and Figures S1, S4, S6 in the Supporting Information), suggesting that the spontaneous insertion of laser-ablated Gd, Tb, Ho, and Er atoms into N_2O to form the $OLn(N_2)$ or OLnNN complexes is the dominant process (reaction 1). Recent studies on the Y and La systems indicated that the reactions start by binding the outer nitrogen atom of N_2O with the metal atom to form a planar intermediate MNNO (M = Y and La) and then rearrange to form a side-bonded intermediate M-(η^2−NN)O and the oxygen atom can further be transferred to form $OM(N_2)$.[2b] Similar isomerizations from LnNNO to $OLn(N_2)$ via Ln-(η^2−NN)O for the Gd, Tb, Ho, and Er reactions have also been obtained and the details could be referred to the Y and La systems.[2b]

$$\mathrm{Ln} + \mathrm{N_2O} \rightarrow \mathrm{LnNNO} \rightarrow \mathrm{Ln\text{-}(\eta^2\text{-}NN)O} \rightarrow \mathrm{OLn(N_2)\ or\ OLnNN} \quad (\mathrm{Ln = Gd, Tb, Ho, and Er}) \quad (1)$$

Recent investigations have shown that laser ablation of metal targets produces not only neutral metal atoms but also metal cations and electrons. Ionic metal complexes can also be formed in the reactions with small molecules.[15] In the present experiments, the $OLnNN^+$ (Ln = Gd, Tb, Ho, and Er) cation complexes appear during sample deposition and increase markedly upon broadband irradiation at the expense of the neutral $OLn(N_2)$ and OLnNN complexes (Figure 1 and Figures S1, S4, and S6 in the Supporting Information), suggesting that the $OLnNN^+$ cations may be generated by photoionization of the neutral OLnNN and $OLn(N_2)$ complexes via radiation in the ablation plume and/or broadband irradiation (reaction 2). It is noted that the $OLnNN^+$ (Ln = Dy, Tm, Yb, and Lu) cations are observed, whereas the corresponding neutral $OLn(N_2)$ and OLnNN complexes are absent (Figures S3, S8, and S9 in the Supporting Information). Moreover, the LnO^+ cations appear in the experiments.[5] Therefore, the reaction of the LnO^+ cations with N_2 may be responsible for the formation of the $OLnNN^+$ cations (reaction 3).

$$\mathrm{OLn(N_2)\ or\ OLnNN} - \mathrm{e^-} \rightarrow \mathrm{OLnNN^+} \quad (2)$$

$$\mathrm{LnO^+} + \mathrm{N_2} \rightarrow \mathrm{OLnNN^+} \quad (3)$$

Together with our earlier work involving early lanthanoid atoms (La−Eu),[2] the neutral $OLn(N_2)$ complexes are observed for La, Ce, Pr, Nd, Sm, Gd, Tb, Ho, and Er, and the neutral OLnNN complexes for Gd, Tb, Ho, and Er in the matrix experiments. The reactions of N_2O with all of the lanthanoid atoms (except for radioactive Pm and for Eu and Yb) produce

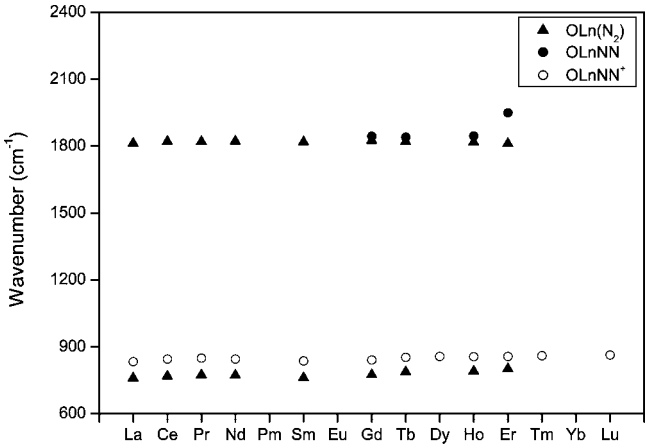

Figure 4. Plot of the experimental N−N (upper dots) and Ln−O (lower dots) stretching frequencies (cm^{-1}) in the $OLn(N_2)$, OLnNN, and $OLnNN^+$ complexes (Ln = lanthanoid atoms).

the $OLnNN^+$ cation complexes. However, no new product is observed in the reactions of N_2O with Eu and Yb, which may be due to the stable electron configurations of Eu ($4f^76s^2$) and Yb ($4f^{14}6s^2$) atoms. As illustrated in Figure 4, the N−N and Ln−O stretching frequencies of the neutral $OLn(N_2)$ complexes show small changes along the series. This trend holds true for the Ln−O stretching frequencies of the $OLnNN^+$ cation complexes.[2] Recent matrix investigations on the reactions of lanthanoid atoms with CO_2 molecules reveal that the early lanthanoid (La−Sm) oxocarbonyl complexes adopt the trans configurations, the europium and ytterbium ones adopt side-on-bonded modes (Eu-(η^2-OC)O and Yb-(η^2-OC)O), and the late lanthanoid (Gd−Lu) ones adopt the cis configurations, exhibiting intriguing structural and bonding trends in the interaction of lanthanoid atoms with CO_2.[9] In contrast, the geometrical structures for the $OLn(N_2)$ and $OLnNN^+$ complexes are very similar. Unlike CO_2, there is no such lanthanoid-ligand trend in the interaction of lanthanoid atoms with N_2O. The present study on the reactions of lanthanoid atoms with N_2O exhibits the difference in chemistry between the semifilled-f-orbital Eu/full-filled-f-orbital Yb and the other lanthanoid elements.

It is noted that the neutral LnO molecules are the major products in the reactions of N_2O with lanthanoid atoms in the gas phase.[1] However, it has been found from the matrix experiments (in the condensed phase) that the yields of the $OLn(N_2)$ molecules are larger than those of the neutral LnO molecules. This suggests the reactivity of gas-phase lanthanoids toward N_2O is quite different from that of condensed phase lanthanoids. It can be found from Table 4 that the Ln−O stretching frequencies of $OLn(N_2)$ are ca. 40 cm^{-1} red-shift from those of LnO and the Ln−O stretching frequencies of $OLnNN^+$ are ca. 5 cm^{-1} red-shift from those of LnO^+. This suggests that the interaction between LnO and NN in $OLn(N_2)$ is stronger than that in $OLnNN^+$, which is consistent with the calculated intensities of these stretching vibrations (Table 3).

As listed in Table 5, there are some electrons in the 5d and 6p orbitals of Ln atoms in the $OLn(N_2)$ complexes, which are similar to the lanthanoid oxocarbonyl complexes. This implies that the formation of $OLn(N_2)$ involves the promotion of 6s and 4f electrons into the metal valence shell. The NBO analyses further reveal that the $OLn(N_2)$ complexes have significant bonding interactions between the 2p orbitals of O and N atoms and the 5d orbitals of Ln atoms. The $OEu(N_2)$, $ODy(N_2)$, $OYb(N_2)$, and $OLu(N_2)$ complexes are absent from the present experimental conditions and hopefully observed in the future experiments with the development of experimental technique.

Conclusions

Reactions of late lanthanoid (Gd−Lu) atoms with N_2O molecules in excess argon have been investigated using matrix-isolation infrared spectroscopy. The $OLn(N_2)$, OLnNN (Ln = Gd, Tb, Ho, and Er), and $OLnNN^+$ (Ln = Gd, Tb, Dy, Ho, Er, Tm, and Lu) complexes have been observed and characterized in an argon matrix on the basis of the isotopic substitution, the N_2O concentration change, and CCl_4-doping experiments, whereas no such species is apparent with Yb. Density functional theory calculations have been performed on the products. The agreement between the experimental and calculated vibrational frequencies, relative absorption intensities, and isotopic shifts supports identification of these new species from the matrix infrared spectra. Together with our earlier work involving early lanthanoid atoms (La−Eu), it has been found that the N−N and Ln−O stretching frequencies of the neutral $OLn(N_2)$ complexes show small changes along the lanthanoid series. This trend holds true for the Ln−O stretching frequencies of the $OLnNN^+$ cation complexes. The present study exhibits the difference in chemistry between the semifilled-f-orbital Eu/full-filled-f-orbital Yb and the other lanthanoid elements.

Acknowledgment. This work was supported by AIST and a Grant-in-Aid for Scientific Research (B) (Grant No. 17350012) from the Ministry of Education, Culture, Sports, Science and Technology (MEXT) of Japan. L.J. is grateful to the Japan Society for Promotion of Science (JSPS) for a postdoctoral fellowship.

Supporting Information Available: The infrared spectra of the Tb, Dy, Ho, Er, Tm, Yb, and Lu reactions. This information is available free of charge via the Internet at http://pubs.acs.org.

References and Notes

(1) Campbell, M. L *J. Chem. Phys.* **1999**, *111*, 562 (Ln + N_2O, in the gas phase).

(2) (a) Zhou, M. F.; Wang, G. J.; Zhao, Y. Y.; Chen, M. H.; Ding, C. F *J. Phys. Chem. A* **2005**, *109*, 5079 (Sc + N_2O, in matrix). (b) Jiang, L.; Xu, Q. *J. Phys. Chem. A* **2008**, *112*, 6289 (Y, La + N_2O, in matrix). (c) Jiang, L.; Xu, Q. *J. Phys. Chem. A* **2008**, *112*, 8690 (Ce, Pr, Nd, Sm, Eu + N_2O, in matrix).

(3) (a) Slater, J. L.; Sheline, R. K.; Lin, K. C.; Weltner, W., Jr. *J. Chem. Phys.* **1971**, *55*, 5129. (b) Slater, J. L.; DeVore, T. C.; Calder, V. *Inorg. Chem.* **1973**, *12*, 1918. (c) Slater, J. L.; DeVore, T. C.; Calder, V. *Inorg. Chem.* **1974**, *13*, 1808. (d) Sheline, R. K.; Slater, J. L. *Angew. Chem., Int. Ed.* **1975**, *14*, 309. (e) Xu, Q.; Jiang, L.; Zou, R. Q. *Chem. Eur. J.* **2006**, *12*, 3226. (f) Zhou, M. F.; Jin, X.; Li, J. *J. Phys. Chem. A* **2006**, *110*, 10206. (g) Jin, X.; Jiang, L.; Xu, Q.; Zhou, M. F. *J. Phys. Chem. A* **2006**, *110*, 12585. (h) Jiang, L.; Jin, X.; Zhou, M. F.; Xu, Q. *J. Phys. Chem. A* **2008**, *112*, 3627 (Ln + CO, in matrix).

(4) Willson, S. P.; Andrews, L. *J. Phys. Chem. A* **1998**, *102*, 10238. (a) Willson, S. P.; Andrews, L. *J. Phys. Chem. A* **1999**, *103*, 1311 (Ln + N_2, in matrix). (b) Zhou, M. F.; Jin, X.; Gong, Y.; Li, J. *Angew. Chem., Int. Ed.* **2007**, *46*, 2911 (Gd + N_2, in matrix).

(5) (a) Andrews, L.; Zhou, M. F.; Chertihin, G. V.; Bauschlicher, C. W., Jr. *J. Phys. Chem. A* **1999**, *103*, 6525 (Y, La + O_2, in matrix). (b) Willson, S. P.; Andrews, L *J. Phys. Chem. A* **1999**, *103*, 3171 (Ce, Pr, Nd, Sm, Eu, Gd + O_2, in matrix). (c) Willson, S. P.; Andrews, L. *J. Phys. Chem. A* **1999**, *103*, 6972 (Tb, Dy, Ho, Er, Tm, Yb, Lu+ O_2, in matrix).

(6) Willson, S. P.; Andrews, L.; Neurock, M *J. Phys. Chem. A* **2000**, *104*, 3446 (Ln + NO, in matrix).

(7) Willson, S. P.; Andrews, L. *J. Phys. Chem. A* **2000**, *104*, 1640 (Ln + H_2, in matrix).

(8) (a) Xu, J.; Zhou, M. F. *J. Phys. Chem. A* **2006**, *110*, 10575. (b) Xu, J.; Jin, X.; Zhou, M. F. *J. Phys. Chem. A* **2007**, *111*, 7105 (Ln + H_2O, in matrix).

(9) Jiang, L.; Zhang, X. B.; Han, S.; Xu, Q. *Inorg. Chem.* **2008**, *47*, 4826 (Ln + CO_2, in matrix).

(10) (a) Burkholder, T. R.; Andrews, L. *J. Chem. Phys.* **1991**, *95*, 8697. (b) Zhou, M. F.; Tsumori, N.; Andrews, L.; Xu, Q. *J. Phys. Chem. A* **2003**, *107*, 2458. (c) Jiang, L.; Xu, Q. *J. Chem. Phys.* **2005**, *122*, 034505. (d) Jiang, L.; Teng, Y. L.; Xu, Q. *J. Phys. Chem. A* **2006**, *110*, 7092.

(11) Frisch, M. J.; Trucks, G. W.; Schlegel, H. B.; Scuseria, G. E.; Robb, M. A.; Cheeseman, J. R.; Montgomery, J. A., Jr.; Vreven, T.; Kudin, K. N.; Burant, J. C.; Millam, J. M.; Iyengar, S. S.; Tomasi, J.; Barone, V.; Mennucci, B.; Cossi, M.; Scalmani, G.; Rega, N.; Petersson, G. A.; Nakatsuji, H.; Hada, M.; Ehara, M.; Toyota, K.; Fukuda, R.; Hasegawa, J.; Ishida, M.; Nakajima, T.; Honda, Y.; Kitao, O.; Nakai, H.; Klene, M.; Li, X.; Knox, J. E.; Hratchian, H. P.; Cross, J. B.; Bakken, V.; Adamo, C.; Jaramillo, J.; Gomperts, R.; Stratmann, R. E.; Yazyev, O.; Austin, A. J.; Cammi, R.; Pomelli, C.; Ochterski, J. W.; Ayala, P. Y.; Morokuma, K.; Voth, G. A.; Salvador, P.; Dannenberg, J. J.; Zakrzewski, V. G.; Dapprich, S.; Daniels, A. D.; Strain, M. C.; Farkas, O.; Malick, D. K.; Rabuck, A. D.; Raghavachari, K.; Foresman, J. B.; Ortiz, J. V.; Cui, Q.; Baboul, A. G.; Clifford, S.; Cioslowski, J.; Stefanov, B. B.; Liu, G.; Liashenko, A.; Piskorz, P.; Komaromi, I.; Martin, R. L.; Fox, D. J.; Keith, T.; Al-Laham, M. A.; Peng, C. Y.; Nanayakkara, A.; Challacombe, M.; Gill, P. M. W.; Johnson, B.; Chen, W.; Wong, M. W.; Gonzalez, C.; Pople, J. A. Gaussian 03, revision B.04; Gaussian, Inc., Pittsburgh, PA, 2003.

(12) (a) Becke, A. D. *Phys. Rev. A* **1988**, *38*, 3098. (b) Perdew, J. P. *Phys. Rev. B* **1986**, *33*, 8822.

(13) (a) McLean, A. D.; Chandler, G. S. *J. Chem. Phys.* **1980**, *72*, 5639. (b) Krishnan, R.; Binkley, J. S.; Seeger, R.; Pople, J. A. *J. Chem. Phys.* **1980**, *72*, 650.

(14) Andrae, D.; Haeussermann, U.; Dolg, M.; Stoll, H.; Preuss, H. *Theor. Chim. Acta* **1990**, *77*, 123.

(15) Zhou, M. F.; Andrews, L.; Bauschlicher, C. W., Jr. *Chem. Rev.* **2001**, *101*, 1931, and references therein.

(16) Darling, J. H.; Ogden, J. S. *J. Chem. Soc., Dalton Trans.* **1972**, 2496.

(17) See, for example, Pyykkö, P *Chem. Rev.* **1988**, *88*, 563. Pepper, M.; Bursten, B. E. *Chem. Rev* **1991**, *91*, 719. Seth, M.; Dolg, M.; Fulde, P.; Schwerdtfeger, P. *J. Am. Chem. Soc.* **1995**, *117*, 6597. Li, J.; Bursten, B. E. *J. Am. Chem. Soc.* **1997**, *119*, 9021.

(18) Adamo, C.; Maldivi, P. *J. Phys. Chem. A* **1998**, *102*, 6812. Dolg, M.; Liu, W.; Kalvoda, S. *Int. J. Quantum Chem.* **2000**, *76*, 359. Maron, L.; Eisenstein, O. *J. Phys. Chem. A* **2000**, *104*, 7140.

(19) Gibson, J. K. *J. Phys. Chem. A* **2003**, *107*, 7891.

(20) de Almeida, K. J.; Cesar, A. *Organometallics* **2006**, *25*, 3407.

JP809549U